SSRG International Journal of Electrical and Electronics Engineering
ISSN: 2348-8379/ https://doi.org/10.14445/23488379/IJEEE-V13I5P104

Volume 13 Issue 5, 33-47, May 2026

Original Article

Machine Learning-driven Design Optimization of Antennas using Linear Regression

Archana Tiwari[1], S. G. Bhele[2], Joydeep Dutt[3], Shruti Dutt[1], Nita Nimbarte[4]

[1]*Electronics Engineering Department, Shri. Ramdeobaba College of Engineering and Management, Nagpur, 440013, India.*
[2]*Electronics & Telecommunication Department, Government College of Engineering Nagpur, India.*
[3]*Senior Technical Advisor, Microsoft, Sydney, Australia.*
[4]*Electronics & Telecommunication Department, Yeshwantrao Chavan College of Engineering, Nagpur, India.*

[1]*Corresponding Author : tiwariar@rknec.edu*

Received: 08 February 2026 Revised: 07 March 2026 Accepted: 06 April 2026 Published: 30 May 2026

Abstract - *The proposed method explores the application of Machine Learning (ML) techniques, specifically Linear Regression, to optimize antenna design for Artificial Intelligence (AI) and Internet of Things (IoT) enabled wireless communication systems. Traditional design methods relying on numerical Electromagnetic (EM) simulations are time-consuming and resource-intensive. The proposed approach leverages ML to predict antenna performance metrics, significantly reducing design time and enhancing accuracy. A Linear Regression model was trained on 300 datasets generated from HFSS simulations, achieving impressive accuracy rates of 91.94% to 97.18% for resonant frequency and 78.69% to 99.77% for return loss. The results demonstrate the potential of ML in streamlining antenna design processes, enabling the development of efficient and compact antennas for AI- and IoT-driven applications. The designed antenna was fabricated on an FR-4 substrate and characterized using a Vector Network Analyzer, validating the effectiveness of the ML-based approach.*

Keywords - *Antenna, Compact, Linear regression, Machine Learning, Optimization.*

1. Introduction

Artificial Intelligence (AI) in wireless communication controls network traffic, forecasts device behavior, and enhances overall system dependability and efficiency [1-3]. The antenna is a crucial component that transmits and receives electromagnetic waves at the center of any wireless communication system. In traditional antenna design methods, Maxwell equations are used, and are solved through the extensive use of numerical simulations using software tools like Finite Element Method (FEM), which is utilized by the High- Frequency Structure Simulator (HFSS), etc. [4, 5]. Even though these simulations are accurate, they need a lot of time and resources. To optimize antenna performance, the iterative design method is used, which usually tests several configurations [6]. Since each iteration necessitates a new simulation, the total design time is increased, and it also requires a lot of processing power. These problems have a possible answer in ML, where an algorithm is used to forecast antenna performance without depending on laborious Simulations [7]. Hence, the antenna design process sped up through ML algorithms, which produce precise predictions. Reduced computational resource requirements from fewer simulations equate to cost savings [8]. The design of an E-shaped antenna using the ML algorithm is proposed in [9], where antennas working at 5 and 5.5 GHz are simulated using Ansoft HFSS software. Researchers discuss the design of reflector array antennas using the Support Vector Machine (SVM) machine learning technique, where the frequency of operation is 25.5 GHz [10]. The proposed design of UWB antennas using the SVM machine learning algorithm, working at 9 GHz, is discussed in [11]. Paper [12] discusses the use of the Bayesian regularization machine learning technique in the construction of antennas (planar inverted-F antenna) using nano magnetic materials, where the frequency of operation is 1 GHz, and simulations were carried out using CST software.

The advanced design methods based on learning to reflect array antennas with the Kriging machine learning algorithm were presented in [13], working at 3.9 GHz. In [14], the design of Nanomagnetic-based antennas (planar inverted-F antenna) using a Neural Network machine learning algorithm at 1 GHz frequency. The design of microstrip-based antennas using ANN/SVM machine learning algorithms was presented in [15]. Paper [16] discusses the design of using an ANN machine learning algorithm, a Slotted Waveguide Array Antenna (SWAA), where the frequency of operation is 78.7 GHz, and simulations carried out using HFSS software. The patch antenna simulated using IE3D software, where an ANN machine learning algorithm is explored, is proposed in [17], where the frequency is 18 to 24 GHz.

This work focuses on optimizing the design of rectangular patch antennas through ML algorithms, specifically linear regression. This paper presents the training of machine learning models to predict important performance metrics like resultant frequency and return loss using data considering antenna designs simulated from HFSS. The aim is to show how ML may simplify the antenna design process to increase its economy and efficiency. A further section in the paper is organized as follows: antenna design methodology, machine learning approach in antenna design, result analysis, and conclusion. Also, the effectiveness of the ML models and the benefits of the proposed methodology are discussed in conclusion.

2. Antenna Design

A rectangular metal patch is positioned on a dielectric substrate with a ground plane on the other side to form a rectangular patch antenna [18]. Due to their simple design and ease of production, rectangular patch antennas are frequently employed in wireless communication. The design parameters, such as the patch's width and length, the dielectric constant of the substrate, and the feed position, significantly influence the antenna's performance with relation to return loss, gain, and bandwidth. Formulas such as resonant frequency (fr), effective dielectric constant (εeff), width of the patch (W), length extension (ΔL), actual length of the patch (L), input impedance (Zin), and return loss ($S11$), Substrate width (Ws), Substrate length (Ls) were used to determine the design specifications of patch and substrate.

Resonant Frequency $fr = \frac{c}{2L\sqrt{\varepsilon r}}$ (1)

Effective Dielectric Constant $\mathfrak{E}eff = \frac{\varepsilon r+1}{2} + \frac{\varepsilon r-1}{2}(1 + 12\frac{h}{W})^{-0.5}$ (2)

Width of the Patch $W = \frac{c}{2fr}\sqrt{\frac{2}{\varepsilon r+1}}$ (3)

Length Extension $\Delta L = 0.412h\frac{(\epsilon eff+0.3)(\frac{W}{h}+0.264)}{(\epsilon eff-0.258)(\frac{W}{h}+0.8)}$ (4)

Actual Length of the Patch $L = \frac{c}{2fr\sqrt{\epsilon eff}} - 2\Delta L$ (5)

Input Impedance $Zin = Zo(\frac{1+\Gamma}{1-\Gamma})$ (6)

Width of the Substrate $Ws = 12h + W$ (7)

Length of the Substrate $Ls = 12h + L$ (8)

Return Loss $S11 = 20|\Gamma|$ (9)

Where c is the speed of light in vacuum, the reflection coefficient is Gamma; the characteristic impedance of the feed line is Zo; and the substrate's relative permittivity is (Ɛr). With the design antenna and its performance for ISM band applications, the rectangular microstrip patch antenna's fundamental construction is considered. The design is targeted for antennas working at 2.45 GHz frequency with the FR4 (4.4 dielectric constant, 1.6 mm thick) substrate material. The rectangular microstrip patch antenna basic structure is shown in Figure 1.

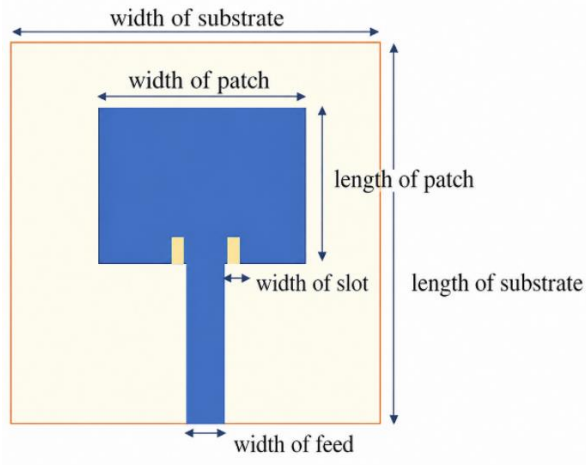

Fig. 1 Rectangular Microstrip Patch Antenna

In the optimization process, there is a requirement to adjust the input parameters of the antenna in the next experiment based on the results of the current experiment to improve the performance of the antenna [19]. The antenna performance can be modified by parametric variations of: patch width, ground plane, substrate height, feed point placement, dielectric constant, loss tangent, probe diameter, and cover/coating. Out of these, the following characteristics are considered for variation: patch width, substrate width, substrate length, slot width, and feed width. The antenna's radiation characteristics are affected by the slot's length, resonant frequency, and bandwidth, which are affected by the substrate's length, and impedance matching and return loss are affected by the slot's width.

3. Machine Learning Approach in Antenna Design

Machine learning algorithms can be broadly categorized into supervised and unsupervised learning; however, in this work, the focus is strictly on supervised regression techniques for antenna design, as illustrated in Figure 2. ML models can predict key performance indicators, significantly reducing the number of required simulations and accelerating the design process [20]. In particular, supervised learning enables the mapping between input parameters-such as antenna dimensions and substrate properties-and output responses like resonant frequency, return loss, and gain [23]. Among these,

linear regression serves as a simple yet effective approach for modeling the relationship between input variables and performance metrics [24]. By leveraging regression-based models, it becomes possible to efficiently approximate antenna behavior and explore design variations within a reduced computational time. The overall methodology involves data generation using HFSS simulations, selection of an appropriate regression model, training using labeled datasets, and subsequent validation and testing, as depicted in Figure 3.

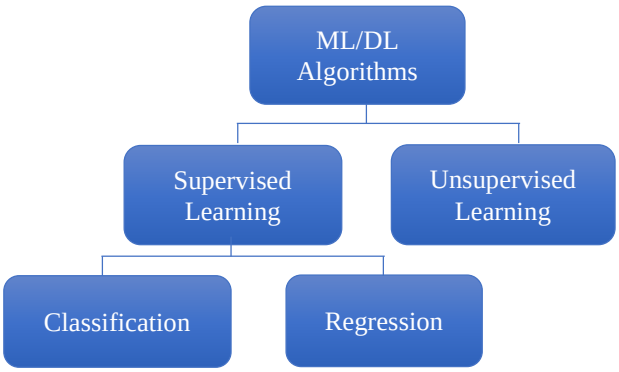

Fig. 2 Flowchart showing different ML algorithms

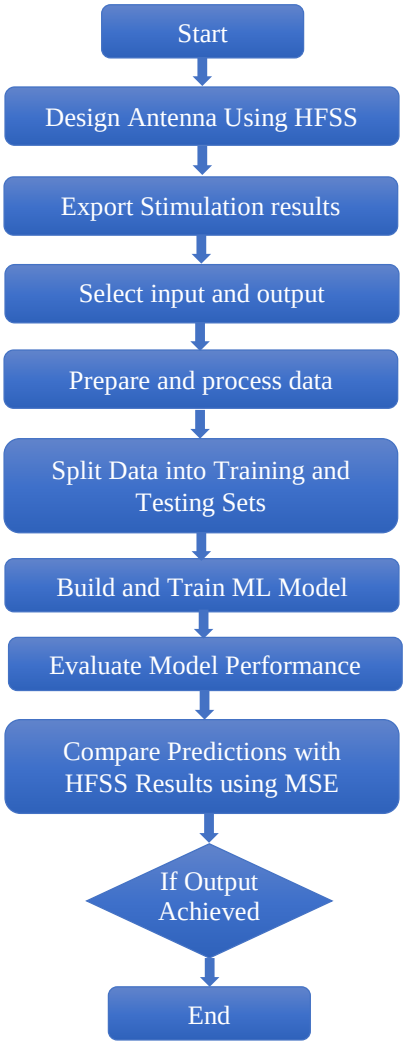

Fig. 3 Process involved for ML in antenna design

3.1. Data Collection

The data collection phase is crucial as it sets the foundation for the entire optimization process. An extensive collection of rectangular patch antenna designs has been created, and the performance parameters that go along with them have been determined using HFSS. In the data collection phase, I meticulously simulated various rectangular patch antenna designs using HFSS. This simulation tool enables the detailed analysis of antenna characteristics using the specified geometry and material properties to solve Maxwell's equations. Each simulation run involved varying the design parameters systematically to cover a broad range of configurations. The HFSS antenna design procedure includes creating a 3D model. The antenna's physical dimensions, the substrate and patch's material properties, boundary conditions, and excitation techniques are established for simulation.

The HFSS simulations provided detailed information on the resonance frequency, radiation patterns, and return loss. These were recorded and organized to form a comprehensive dataset essential for training and validating the ML models. The primary performance metrics gathered from these simulations included the resonant frequency (GHz), which indicates the frequency at which the antenna efficiently radiates, and the return loss (S11) dB, which measures the amount of power reflected back into the system, reflecting the quality of impedance matching as shown in Table 1. This comprehensive dataset served as the training and testing data for the ML models. The antenna performance parameters that were considered for variation were: patch width, substrate width, substrate length, slot width, and feed width, where the length of the patch (L=29.73 *mm*) was considered constant.

Table 1. Parametric variations of antenna parameters with simulation results

Experiments	Width of Patch (mm)	Width of Substrate (mm)	Length of Substrate (mm)	Width of Slot (mm)	Width of Feed (mm)	Resultant Frequency (GHz)	Return Loss (dB)
M1	55.89	70.2	53.83	0.5	2.27	2.58	-18.99
M2	55.89	58.5	49.07	0.37	1.515	2.49	-12.93
M3	55.89	46.8	44.17	0.25	4.545	2.32	-19.98
M4	55.89	35.1	39.26	0.75	3.79	2.48	-18.94
M5	55.89	23.4	58.89	0.62	3.03	2.66	-22.45
M6	48.37	60.37	49.66	0.9375	3.79	2.34	-14.96
M7	48.37	57.4	46.85	0.78125	3.03	2.56	-22.19
M8	48.37	54.435	44.044	0.625	2.27	2.26	-8.08
M9	48.37	51.4675	41.235	1.25	1.515	2.32	-10.89
M10	48.37	48.5	52.47	1.094	4.545	2.3	-29.79
M11	46.57	70.2	49.07	0.25	8.97	2.43	-22.46
M12	46.57	58.5	44.17	0.75	8.22	2.43	-19.72
M13	46.57	46.8	39.26	0.62	7.47	2.43	-14.01
M14	46.57	35.1	58.89	0.5	6.72	3.98	-28.34
M15	46.57	23.4	53.83	0.37	5.98	5.06	-24.23
M16	44.71	62.71	53.89	0.25	6.72	2.45	-10.59
M17	44.71	62.71	53.89	0.25	5.98	2.45	-7
M18	44.71	57.12	51.64	0.37	8.97	2.46	-7.41
M19	44.71	57.12	49.39	0.37	8.22	2.54	-3.49
M20	44.71	51.53	49.39	0.5	7.47	2.44	-32.66
M21	44.71	51.53	44.89	0.5	1.515	2.3	-7.64
M22	44.71	45.94	47.14	0.62	4.545	2.36	-23.7
M23	44.71	45.94	40.39	0.62	3.79	2.36	-16.44
M24	44.71	45	44.89	0.75	3.03	2.38	-14.39
M25	44.71	45	36	0.75	2.27	2.4	-10.76
M26	43.29	45.39	36.89	0.094	8.22	2.48	-7.53
M27	43.29	44.92	36.43	0.078	7.47	2.48	-4.03
M28	43.29	44.44	35.9	0.0625	6.72	2.57	-2.8
M29	43.29	43.97	35.5	0.125	5.98	2.46	-11.77
M30	43.29	43.5	37.36	0.11	8.97	2.46	-17.39
M31	42.324	60.37	46.85	0.625	3.03	2.42	-23.81
M32	42.324	57.4	44.044	1.25	5.98	4.91	-34.12

M33	42.324	54.435	41.235	1.094	2.27	2.4	-29.32
M34	42.324	51.4675	52.47	0.9375	8.97	4.83	-20.66
M35	42.324	48.5	49.66	0.78125	8.22	2.5	-9.39
M36	41.91	62.71	51.64	0.5	1.515	2.38	-8.91
M37	41.91	57.12	49.39	0.62	7.47	2.5	-7.5
M38	41.91	51.53	47.14	0.75	6.72	4.86	-15.08
M39	41.91	45.94	44.89	0.25	4.545	2.44	-28.71
M40	40.35	40.35	53.89	0.37	3.79	2.42	-23.69
M41	39.52	51.52	40.125	0.5	7.47	2.63	-1.86
M42	39.52	45.08	37.25	0.37	6.72	2.53	-5.15
M43	39.52	38.64	34.375	0.25	5.98	2.54	-3.55
M44	39.52	32.2	31.5	0.75	8.97	2.54	-3.81
M45	39.52	25.76	43	0.62	8.22	2.55	-2.23
M46	39.12	62.71	49.39	0.75	4.545	2.58	-12.7
M47	39.12	62.71	49.39	0.5	3.79	2.54	-10.96
M48	39.12	57.12	47.14	0.25	3.03	2.48	-11.8
M49	39.12	57.12	44.89	0.62	2.27	2.48	-20.02
M50	39.12	51.53	44.89	0.37	1.515	2.44	-24.93
M51	39.12	51.53	40.39	0.75	2.27	2.58	-18.99
M52	39.12	45.94	53.89	0.5	1.515	2.58	-10.89
M53	39.12	45.94	36	0.25	4.545	2.32	-19.98
M54	39.12	40.35	53.89	0.37	3.79	2.48	-18.94
M55	39.12	40.35	51.64	0.62	3.03	2.66	-22.45
M56	37.88	45.39	36.43	0.0625	3.79	2.34	-14.96
M57	37.88	44.92	35.9	0.125	3.03	2.56	-22.19
M58	37.88	44.44	35.5	0.11	2.27	2.26	-8.08
M59	37.88	43.97	37.36	0.094	1.515	2.32	-10.89
M60	37.88	43.5	36.89	0.078	4.545	2.3	-29.79
M61	37.26	70.2	44.17	0.62	8.97	2.43	-22.46
M62	37.26	58.5	39.26	0.5	8.22	2.43	-19.72
M63	37.26	46.8	58.89	0.37	7.47	2.43	-14.01
M64	37.26	35.1	53.83	0.25	6.72	3.98	-28.34
M65	37.26	23.4	49.07	0.75	5.98	5.06	-24.23
M66	36.32	62.71	47.14	0.37	6.72	2.45	-10.59
M67	36.32	57.12	44.89	0.5	5.98	2.45	-7
M68	36.32	51.53	53.89	0.62	8.97	2.46	-7.41
M69	36.32	45.94	51.64	0.75	8.22	2.54	-3.49
M70	36.32	40.35	47.14	0.25	7.47	2.44	-32.66
M71	36.2775	60.37	44.044	1.094	1.515	2.3	-7.64
M72	36.2775	57.4	41.235	0.9375	4.545	2.36	-23.7
M73	36.2775	54.435	52.47	0.78125	3.79	2.36	-16.44
M74	36.2775	51.4675	49.66	0.625	3.03	2.38	-14.39
M75	36.2775	48.5	46.85	1.25	2.27	2.4	-10.76
M76	34.58	51.52	37.25	0.25	8.22	2.48	-7.53
M77	34.58	45.08	34.375	0.75	7.47	2.48	-4.03
M78	34.58	38.64	31.5	0.62	6.72	2.57	-2.8
M79	34.58	32.2	43	0.5	5.98	2.46	-11.77
M80	34.58	25.76	40.125	0.37	8.97	2.46	-17.39
M81	33.53	62.71	44.89	0.75	3.03	2.42	-23.81
M82	33.53	62.71	44.89	0.62	5.98	4.91	-34.12

M83	33.53	57.12	53.89	0.75	2.27	2.4	-29.32
M84	33.53	57.12	40.39	0.25	8.97	4.83	-20.66
M85	33.53	51.53	51.64	0.25	8.22	2.5	-9.39
M86	33.53	51.53	36	0.37	1.515	2.38	-8.91
M87	33.53	45.94	53.89	0.5	7.47	2.5	-7.5
M88	33.53	45.94	49.39	0.37	6.72	4.86	-15.08
M89	33.53	40.35	49.39	0.62	4.545	2.44	-28.71
M90	33.53	40.35	47.14	0.5	3.79	2.42	-23.69
M91	32.47	45.39	35.9	0.11	7.47	2.63	-1.86
M92	32.47	44.92	35.5	0.094	6.72	2.53	-5.15
M93	32.47	44.44	37.36	0.078	5.98	2.54	-3.55
M94	32.47	43.97	36.89	0.0625	8.97	2.54	-3.81
M95	32.47	43.5	36.43	0.125	8.22	2.55	-2.23
M96	30.2313	60.37	41.235	0.78125	4.545	2.58	-12.7
M97	30.2313	57.4	52.47	0.625	3.79	2.54	-10.96
M98	30.2313	54.435	49.66	1.25	3.03	2.48	-11.8
M99	30.2313	51.4675	46.85	1.094	2.27	2.48	-20.02
M100	30.2313	48.5	44.044	0.9375	1.515	2.44	-24.93
M101	29.64	51.52	34.375	0.62	2.27	2.58	-18.99
M102	29.64	45.08	31.5	0.5	1.515	2.58	-10.89
M103	29.64	38.64	43	0.37	4.545	2.32	-19.98
M104	29.64	32.2	40.125	0.25	3.79	2.48	-18.94
M105	29.64	25.76	37.25	0.75	3.03	2.66	-22.45
M106	27.94	70.2	39.26	0.37	3.79	2.34	-14.96
M107	27.94	62.71	40.39	0.37	3.03	2.56	-22.19
M108	27.94	58.5	58.89	0.25	2.27	2.26	-8.08
M109	27.94	57.12	36	0.5	1.515	2.32	-10.89
M110	27.94	51.53	53.89	0.62	4.545	2.3	-29.79
M111	27.94	46.8	53.83	0.75	8.97	2.43	-22.46
M112	27.94	45.94	49.39	0.75	8.22	2.43	-19.72
M113	27.94	40.35	44.89	0.25	7.47	2.43	-14.01
M114	27.94	35.1	49.07	0.62	6.72	3.98	-28.34
M115	27.94	23.4	44.17	0.5	5.98	5.06	-24.23
M116	27.05	45.39	35.5	0.078	6.72	2.45	-10.59
M117	27.05	44.92	37.36	0.0625	5.98	2.45	-7
M118	27.05	44.44	36.89	0.125	8.97	2.46	-7.41
M119	27.05	43.97	36.43	0.11	8.22	2.54	-3.49
M120	27.05	43.5	35.9	0.094	7.47	2.44	-32.66
M121	24.7	51.52	31.5	0.37	1.515	2.3	-7.64
M122	24.7	45.08	43	0.25	4.545	2.36	-23.7
M123	24.7	38.64	40.125	0.75	3.79	2.36	-16.44
M124	24.7	32.2	37.25	0.62	3.03	2.38	-14.39
M125	24.7	25.76	34.375	0.5	2.27	2.4	-10.76
M126	24.185	60.37	52.47	1.25	8.22	2.48	-7.53
M127	24.185	57.4	49.66	1.094	7.47	2.48	-4.03
M128	24.185	54.435	46.85	0.9375	6.72	2.57	-2.8
M129	24.185	51.4675	44.044	0.78125	5.98	2.46	-11.77
M130	24.185	48.5	41.235	0.625	8.97	2.46	-17.39
M131	22.35	62.71	36	0.62	3.03	2.42	-23.81
M132	22.35	57.12	53.89	0.75	5.98	4.91	-34.12

M133	22.35	51.53	49.39	0.25	2.27	2.4	-29.32
M134	22.35	45.94	44.89	0.37	8.97	4.83	-20.66
M135	22.35	40.35	40.39	0.5	8.22	2.5	-9.39
M136	21.645	45.39	37.36	0.125	1.515	2.38	-8.91
M137	21.645	44.92	36.89	0.11	7.47	2.5	-7.5
M138	21.645	44.44	36.43	0.094	6.72	4.86	-15.08
M139	21.645	43.97	35.9	0.078	4.545	2.44	-28.71
M140	21.645	43.5	35.5	0.0625	3.79	2.42	-23.69
M141	19.76	51.52	43	0.75	7.47	2.63	-1.86
M142	19.76	45.08	40.125	0.62	6.72	2.53	-5.15
M143	19.76	38.64	37.25	0.5	5.98	2.54	-3.55
M144	19.76	32.2	34.375	0.37	8.97	2.54	-3.81
M145	19.76	25.76	31.5	0.25	8.22	2.55	-2.23
M146	18.63	70.2	58.89	0.75	4.545	2.58	-12.7
M147	18.63	58.5	53.83	0.62	3.79	2.54	-10.96
M148	18.63	46.8	49.07	0.5	3.03	2.48	-11.8
M149	18.63	35.1	44.17	0.37	2.27	2.48	-20.02
M150	18.63	23.4	39.26	0.25	1.515	2.44	-24.93
M151	18.63	23.4	39.26	0.25	1.515	2.44	-24.93
M152	18.63	23.4	39.26	0.25	1.515	2.44	-24.93
M153	55.89	58.5	49.07	0.37	1.515	2.58	-10.89
M154	55.89	58.5	49.07	0.37	1.515	2.58	-10.89
M155	46.57	35.1	58.89	0.5	1.515	2.32	-10.89
M156	46.57	35.1	58.89	0.5	1.515	2.32	-10.89
M157	37.26	70.2	44.17	0.62	1.515	2.3	-7.64
M158	37.26	70.2	44.17	0.62	1.515	2.3	-7.64
M159	27.94	46.8	53.83	0.75	1.515	2.38	-8.91
M160	27.94	46.8	53.83	0.75	1.515	2.38	-8.91
M161	27.94	58.5	58.89	0.25	2.27	2.4	-29.32
M162	27.94	58.5	58.89	0.25	2.27	2.4	-29.32
M163	18.63	35.1	44.17	0.37	2.27	2.48	-20.02
M164	18.63	35.1	44.17	0.37	2.27	2.48	-20.02
M165	55.89	70.2	53.83	0.5	2.27	2.58	-18.99
M166	55.89	70.2	53.83	0.5	2.27	2.58	-18.99
M167	46.57	46.8	39.26	0.62	2.27	2.26	-8.08
M168	46.57	46.8	39.26	0.62	2.27	2.26	-8.08
M169	37.26	23.4	49.07	0.75	2.27	2.4	-10.76
M170	37.26	23.4	49.07	0.75	2.27	2.4	-10.76
M171	37.26	35.1	53.83	0.25	3.03	2.38	-14.39
M172	37.26	35.1	53.83	0.25	3.03	2.38	-14.39
M173	27.94	70.2	39.26	0.37	3.03	2.42	-23.81
M174	27.94	70.2	39.26	0.37	3.03	2.42	-23.81
M175	18.63	46.8	49.07	0.5	3.03	2.48	-11.8
M176	18.63	46.8	49.07	0.5	3.03	2.48	-11.8
M177	55.89	23.4	58.89	0.62	3.03	2.66	-22.45
M178	55.89	23.4	58.89	0.62	3.03	2.66	-22.45
M179	46.57	58.5	44.17	0.75	3.03	2.56	-22.19
M180	46.57	58.5	44.17	0.75	3.03	2.56	-22.19
M181	19.76	25.76	31.5	0.25	3.25	2.5	-4.1
M182	39.52	45.08	37.25	0.37	3.25	2.4	-9.9

M183	34.58	32.2	43	0.5	3.25	2.4	-11.6
M184	29.64	51.52	34.375	0.62	3.25	2.5	-4.7
M185	24.7	38.64	40.125	0.75	3.25	2.5	-9.65
M186	46.57	70.2	49.07	0.25	3.79	2.34	-14.96
M187	46.57	70.2	49.07	0.25	3.79	2.34	-14.96
M188	37.26	46.8	58.89	0.37	3.79	2.36	-16.44
M189	37.26	46.8	58.89	0.37	3.79	2.36	-16.44
M190	27.94	23.4	44.17	0.5	3.79	2.42	-23.69
M191	27.94	23.4	44.17	0.5	3.79	2.42	-23.69
M192	18.63	58.5	53.83	0.62	3.79	2.54	-10.96
M193	18.63	58.5	53.83	0.62	3.79	2.54	-10.96
M194	55.89	35.1	39.26	0.75	3.79	2.48	-18.94
M195	55.89	35.1	39.26	0.75	3.79	2.48	-18.94
M196	21.645	43.5	35.5	0.0625	4	2.42	-23.69
M197	43.29	44.92	36.43	0.078	4	2.43	-18.46
M198	37.88	43.97	37.36	0.094	4	2.43	-17
M199	32.47	45.39	35.9	0.11	4	2.83	-0.7
M200	27.05	44.44	36.89	0.125	4	2.445	-9.99
M201	24.7	45.08	43	0.25	4.0625	2.5	-10.3
M202	19.76	32.2	34.375	0.37	4.0625	2.5	-8.43
M203	39.52	51.52	40.125	0.5	4.0625	2.4	-10.1
M204	34.58	38.64	31.5	0.62	4.0625	2.5	-6.58
M205	29.64	25.76	37.25	0.75	4.0625	2.4	-5.8
M206	55.89	46.8	44.17	0.25	4.545	2.32	-19.98
M207	55.89	46.8	44.17	0.25	4.545	2.32	-19.98
M208	46.57	23.4	53.83	0.37	4.545	2.3	-29.79
M209	46.57	23.4	53.83	0.37	4.545	2.3	-29.79
M210	37.26	58.5	39.26	0.5	4.545	2.36	-23.7
M211	37.26	58.5	39.26	0.5	4.545	2.36	-23.7
M212	27.94	35.1	49.07	0.62	4.545	2.44	-28.71
M213	27.94	35.1	49.07	0.62	4.545	2.44	-28.71
M214	18.63	70.2	58.89	0.75	4.545	2.58	-12.7
M215	18.63	70.2	58.89	0.75	4.545	2.58	-12.7
M216	29.64	32.2	40.125	0.25	4.875	2.4	-11.7
M217	24.7	51.52	31.5	0.37	4.875	2.5	-5.5
M218	19.76	38.64	37.25	0.5	4.875	2.5	-9.11
M219	39.52	25.76	43	0.62	4.875	2.4	-15
M220	34.58	45.08	34.375	0.75	4.875	2.4	-5.62
M221	24.185	48.5	41.235	0.625	4.925	2.52	-2.68
M222	48.37	57.4	46.85	0.78125	4.925	2.42	-10.54
M223	42.324	51.4675	52.47	0.9375	4.925	2.44	-8
M224	36.2775	60.37	44.044	1.094	4.925	2.45	-5.65
M225	30.2313	54.435	49.66	1.25	4.925	2.47	-3.94
M226	27.05	44.92	37.36	0.0625	5	2.435	-8.8
M227	21.645	43.97	35.9	0.078	5	3.08	-1.15
M228	43.29	45.39	36.89	0.094	5	2.43	-20.89
M229	37.88	44.44	35.5	0.11	5	2.765	-0.78
M230	32.47	43.5	36.43	0.125	5	2.44	-13.44
M231	34.58	51.52	37.25	0.25	5.6875	2.5	-10.1
M232	29.64	38.64	43	0.37	5.6875	2.5	-10.52

M233	24.7	25.76	34.375	0.5	5.6875	2.5	-5.9
M234	19.76	45.08	40.125	0.62	5.6875	2.5	-9.8
M235	39.52	32.2	31.5	0.75	5.6875	2.5	-9.5
M236	22.35	51.53	49.39	0.25	5.98	2.54	-3.55
M237	27.94	62.71	40.39	0.37	5.98	4.91	-34.12
M238	33.53	45.94	53.89	0.5	5.98	2.46	-11.77
M239	39.12	57.12	44.89	0.62	5.98	2.45	-7
M240	44.71	45	36	0.75	5.98	5.06	-24.23
M241	32.47	43.97	36.89	0.0625	6	2.435	-11.21
M242	27.05	45.39	35.5	0.078	6	2.955	-1.13
M243	21.645	44.44	36.43	0.094	6	2.45	-8.06
M244	43.29	43.5	37.36	0.11	6	2.43	-23.25
M245	37.88	44.92	35.9	0.125	6	2.75	-2.05
M246	30.2313	57.4	52.47	0.625	6.16	2.48	-3.8
M247	24.185	51.4675	44.044	0.78125	6.16	2.5	-2.57
M248	48.37	60.37	49.66	0.9375	6.16	2.43	-11.155
M249	42.324	54.435	41.235	1.094	6.16	3.2	-6.74
M250	36.2775	48.5	46.85	1.25	6.16	2.46	-7.14
M251	39.52	38.64	34.375	0.25	6.5	2.4	-9.1
M252	34.58	25.76	40.125	0.37	6.5	2.4	-8.9
M253	29.64	45.08	31.5	0.5	6.5	2.5	-6.8
M254	24.7	32.2	37.25	0.62	6.5	2.5	-14.1
M255	19.76	51.52	43	0.75	6.5	2.5	-10.4
M256	27.94	40.35	44.89	0.25	6.72	4.86	-15.08
M257	33.53	51.53	36	0.37	6.72	2.57	-2.8
M258	39.12	62.71	49.39	0.5	6.72	2.45	-10.59
M259	44.71	45.94	40.39	0.62	6.72	3.98	-28.34
M260	22.35	57.12	53.89	0.75	6.72	2.53	-5.15
M261	37.88	45.39	36.43	0.0625	7	2.435	-13.5
M262	32.47	44.44	37.36	0.078	7	2.435	-14.26
M263	27.05	43.5	35.9	0.094	7	2.945	-1.5
M264	21.645	44.92	36.89	0.11	7	2.45	-8.9
M265	43.29	43.97	35.5	0.125	7	2.7	-1.5
M266	36.2775	51.4675	49.66	0.625	7.387	2.465	-6.8
M267	30.2313	60.37	41.235	0.78125	7.387	3.17	-5.06
M268	24.185	54.435	46.85	0.9375	7.387	2.5	-2.82
M269	48.37	48.5	52.47	1.094	7.387	2.44	-18.63
M270	42.324	57.4	44.044	1.25	7.387	2.45	-9.9
M271	33.53	57.12	40.39	0.25	7.47	2.48	-4.03
M272	39.12	40.35	53.89	0.37	7.47	2.44	-32.66
M273	44.71	51.53	44.89	0.5	7.47	2.43	-14.01
M274	22.35	62.71	36	0.62	7.47	2.63	-1.86
M275	27.94	45.94	49.39	0.75	7.47	2.5	-7.5
M276	43.29	44.44	35.9	0.0625	8	2.63	-2.3
M277	37.88	43.5	36.89	0.078	8	2.435	-19.46
M278	32.47	44.92	35.5	0.094	8	2.845	-1.19
M279	27.05	43.97	36.43	0.11	8	2.45	-12.9
M280	21.645	45.39	37.36	0.125	8	2.455	-9.67
M281	39.12	45.94	36	0.25	8.22	2.54	-3.49
M282	44.71	57.12	49.39	0.37	8.22	2.43	-19.72

M283	22.35	40.35	40.39	0.5	8.22	2.55	-2.23
M284	27.94	51.53	53.89	0.62	8.22	2.5	-9.39
M285	33.53	62.71	44.89	0.75	8.22	2.48	-7.53
M286	42.324	60.37	46.85	0.625	8.62	2.45	-10.458
M287	36.2775	54.435	52.47	0.78125	8.62	2.475	-7.39
M288	30.2313	48.5	44.044	0.9375	8.62	2.5	-5.26
M289	24.185	57.4	49.66	1.094	8.62	2.54	-3.12
M290	48.37	51.4675	41.235	1.25	8.62	3.19	-6.61
M291	44.71	62.71	53.89	0.25	8.97	2.43	-22.46
M292	22.35	45.94	44.89	0.37	8.97	2.54	-3.81
M293	27.94	57.12	36	0.5	8.97	4.83	-20.66
M294	33.53	40.35	49.39	0.62	8.97	2.46	-17.39
M295	39.12	51.53	40.39	0.75	8.97	2.46	-7.41
M296	48.37	54.435	44.044	0.625	9.85	2.435	-19.94
M297	42.324	48.5	49.66	0.78125	9.85	2.45	-15.43
M298	36.2775	57.4	41.235	0.9375	9.85	3.34	-6.557
M299	30.2313	51.4675	46.85	1.094	9.85	2.5062	-6.37
M300	24.185	60.37	52.47	1.25	9.85	2.55	-3.45

3.2. ML Model Training

The ML model offers a quick and less resource-intensive method of predicting antenna performance measures because it is trained using data produced by HFSS simulations. The use of ML speeds up the antenna design process in contrast to conventional approaches. The dataset is split into 80% for training and 20% for testing in order to guarantee that the model learns the correlations between input parameters and performance measures from a sizable portion of the data while still being verified on untested designs. By fitting a linear equation to observed data, a linear regression model is a statistical technique used to represent the connection between a dependent variable and one or more independent variables. One independent variable is used in the most basic version, known as simple linear regression, and the model is represented by equation 10, which is displayed below:

$$Y = \beta_0 + \beta_1 x + \varepsilon \quad (10)$$

where β0 is the y-intercept, β1 is the slope of the line, ε is the error term, Y is the dependent variable, and x is the independent variable. The objective is to determine the values of β0 and β1 that minimize the total squared discrepancies between the model's projected values and the actual values. Most commonly, the least squares method is used to do this.

Once the model is fitted, metrics such as the coefficient of determination R^2 can be used to evaluate the overall fit of the model, forecast the dependent variable for given values of the independent variable or variables, and analyze the strength and direction of the association. The study involved adjusting the following parameters: the width of the feed, the width of the patch, the width of the substrate, the length of the substrate, and the width of the slot. The performance of the antenna is directly affected by these factors, which also include return loss and resonance frequency. The resulting frequency, or the frequency at which the antenna resonates, and the return loss (S11), or the amount of impedance mismatch and a measure of the antenna's power radiating efficiency, are the expected outputs of the ML model. In this paper, a total of 300 datasets generated from HFSS simulation were used to train the linear regression ML model, where 80% of the data (M1-M240 of Table 1) was used for training, and 20% (M241-M300 of Table 1) was used for testing the model.

3.3. Validation

Another set of test data from V1–V5, as indicated in Tables 2 and 3, is taken into consideration for validating the trained ML linear regression models. The input parameters for this data include the width of the patch, the width of the substrate, the length of the substrate, the width of the slot, and the width of the feed. The ML linear regression model was trained with these inputs in order to predict two crucial outputs: return loss and resonant frequency. Table 1 displays the detailed dataset of antenna performance that was used to train the model using data collected from HFSS simulations. The resonant frequency predicted outputs from the ML linear regression model for validation experiments V1-V5 range from approximately 2.53 GHz to 2.68 GHz (in the ISM band). Next, the Mean Squared Error (MSE) values are computed using Equation (11)'s formula:

$$\text{Mean Squared error } MSE = \frac{1}{N}\sum_{i=1}^{N}(fi - Yi)^2 \quad (11)$$

where Yi is the actual value for data point i, fi is the value determined by the model, and N is the total number of data points. V1 had an MSE of 0.0081, indicating a high accuracy of 96.31%, while V5 had an MSE of 0.0196, with an accuracy of 94.31% as presented in Table 2. These results demonstrate

that the models are capable of accurately predicting the resonant frequency, with maximum accuracy observed at 97.18% and minimum accuracy at 91.94%. Similarly, the return loss predicted for the same validating data (V1-V5) is presented in Table 3. The MSE and accuracy are also shown, and it has been observed that using a linear regression model, the maximum accuracy achieved for return loss prediction is 99.77%. The M2 antenna design is fabricated on a commercially accessible, inexpensive FR-4 substrate with a dielectric constant of 4.4 and a loss tangent of 0.02. The prototype was characterized with the use of a Vector Network Analyzer from Keysight Technologies with a 50 Ω SMA connector to the microstrip feed line. Figure 4: The fabricated prototype measurement setup. Figure 5 and Table 4 depict the fabricated prototype measurement comparison with simulated results.

Table 2. Validation for resonant frequency

	Input					Output		Validation			
	Patch Width (mm)	Substrate Width (mm)	Substrate Length (mm)	Slot width (mm)	Feed width (mm)	Resonant Frequency output from HFSS (GHz)	Resonant Frequency output from ML model prediction (GHz)	MSE	RMSE	R^2	Accuracy (%)
V1	17	20	38	0.2	1.5	2.44	2.53	0.0081	0.090	0.9631	96.31
V2	18	19	35	0.3	1.6	2.48	2.68	0.0040	0.063	0.9194	91.94
V3	16	18	37	0.2	1.4	2.48	2.55	0.0049	0.070	0.9718	97.18
V4	17.5	19.5	36	0.3	1.45	2.46	2.64	0.0324	0.180	0.9268	92.68
V5	16.5	20	36.5	0.25	1.55	2.46	2.6	0.0196	0.140	0.9431	94.31

Table 3. Validation for return loss

	Input					Output		Validation			
	Patch Width (mm)	Substrate Width (mm)	Substrate Length (mm)	Slot width (mm)	Feed width (mm)	Resonant Frequency output from HFSS (GHz)	Resonant Frequency output from ML model prediction (GHz)	MSE	RMSE	R^2	Accuracy (%)
V1	17	20	38	0.2	1.5	-12.77	-17.74	0.0009	0.030	0.9977	99.77
V2	18	19	35	0.3	1.6	-13.94	-16.91	8.8209	2.970	0.7869	78.69
V3	16	18	37	0.2	1.4	-16.69	-17.71	1.0404	1.020	0.9389	93.89
V4	17.5	19.5	36	0.3	1.45	-17.84	-16.88	0.9216	0.960	0.9462	94.62
V5	16.5	20	36.5	0.25	1.55	-12.68	-17.01	0.4489	0.670	0.9472	94.72

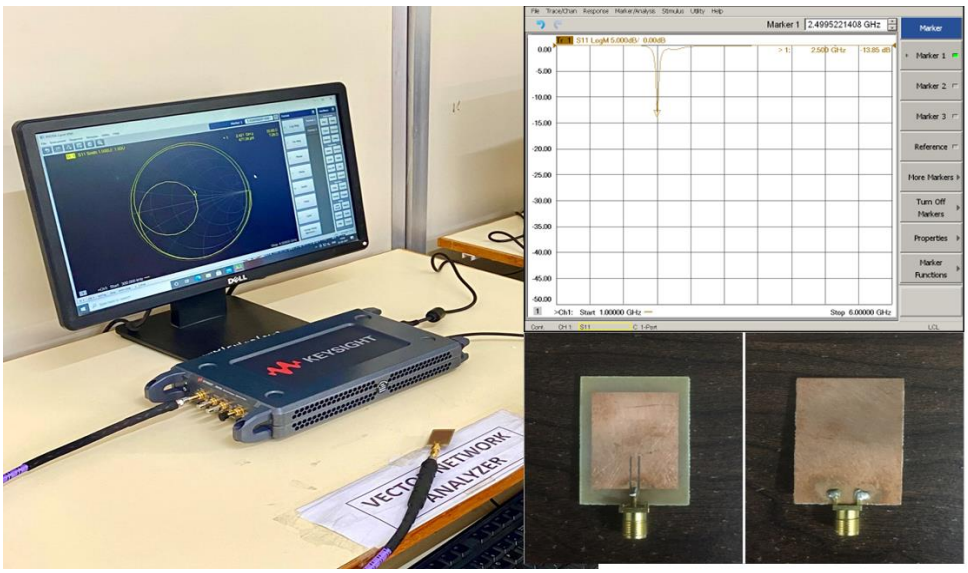

Fig. 4 M2 antenna design measurement setup

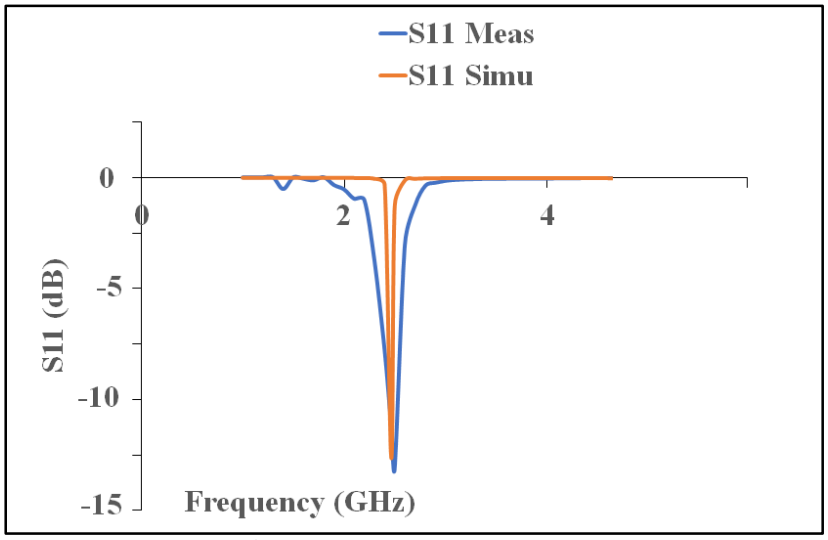

Fig. 5 Comparison of simulated antenna M2 design and measurement results

Table 4. Comparison of simulated antenna M2 design and measurement results

M2 Design	Resonant frequency (GHz)	Bandwidth (%)	Return loss (dB)	Real part of Impedance measured on Smith Chart (ohms)
Simulated Results	2.49	2.06	-12.93	47.26
Measured Results	2.50	3.46	-13.85	49.9

4. Results and Discussion

The validation results demonstrate that the Linear Regression model provides accurate and reliable predictions for resonant frequency and return loss, indicating that it effectively captures the underlying relationship between antenna geometrical parameters and electromagnetic performance. This suitability arises from the fact that, within the considered design space, the variation of key antenna parameters (such as patch dimensions, substrate size, and feed characteristics) exhibits a predominantly linear or near-linear dependency on performance metrics, as commonly observed in microstrip antenna theory. By approximating this relationship through a linear mapping, the model is able to generalize well across the dataset without overfitting, ensuring both stability and interpretability. Furthermore, the low prediction error metrics (e.g., MSE and RMSE) and high coefficient of determination (R^2) values obtained during validation confirm that the model explains a significant proportion of variance in the HFSS-simulated data. The comparative plots in Figure 6, showing close agreement between predicted and simulated values for resonant frequency and return loss across models (V1–V5), provide additional empirical evidence of the model's effectiveness. These observations collectively justify the use of Linear Regression as a computationally efficient and sufficiently accurate approach for modeling and optimizing antenna performance within the defined parameter range. The y-axis of the resonant frequency graph indicates the resonant frequency in GHz, while the x-axis shows the V1–V5 trials. Both the anticipated values from the ML model and the outcomes of the HFSS simulation are included in the shown points. For the majority of configurations, the HFSS outcomes and the ML forecasts closely match, indicating the great accuracy of the models. As an example, V1 produced a resonant frequency prediction of 2.53 GHz, which was 96.31% accurate when compared to the HFSS result of 2.44 GHz.

In a similar vein, V3 achieved 97.18% accuracy in predicting a resonance frequency of 2.55 GHz compared to the HFSS value of 2.48 GHz. In the return loss graph, the x-axis again represents V1-V5 experiments, while the y-axis shows the return loss in dB. The graph compares the return loss values obtained from HFSS simulations with those predicted by the ML models. The accuracy of these predictions is evidenced by the proximity of the ML-predicted values to the HFSS results. For example, V1 predicted a return loss of -12.74 dB compared to the HFSS value of -12.77 dB, demonstrating an accuracy of 99.77%. However, V2's anticipated return loss of -16.91 dB differed more from the HFSS value of -13.94 dB, leading to a lower accuracy of 78.69%. The high accuracy rates and low mean squared error values for most predictions confirm the models' capability to estimate resonant frequency and return loss reliably, thus validating their application in antenna design optimization. The comparative analysis of the proposed model with existing literature is also presented in Table 5.

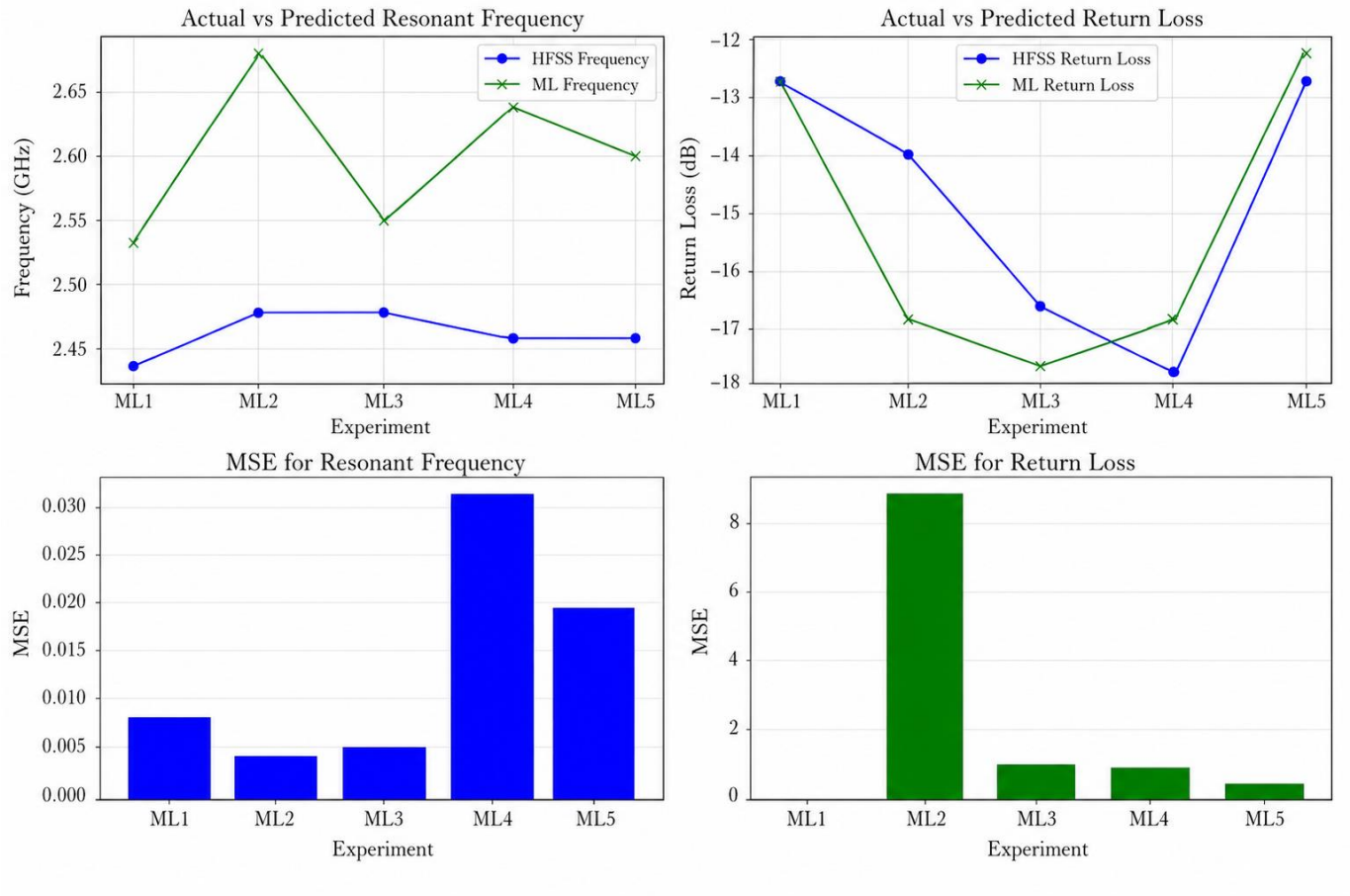

Fig. 6 Comparative performance analysis of the trained model compared to HFSS simulation results

Table 5. Comparison with existing literature

References	Type of Antenna	Frequency of operation (GHz)	ML algorithm	Simulation tool
[9]	E-shaped patch	5 and 5.5	Kriging	HFSS
[10]	Reflector array	25.5	SVM	MoM LP
[12]	Planar inverted-F antenna (PIFA)	1	Bayesian regularization	CST
[14]	PIFA	1	Neural Network	CST
[16]	Slotted waveguide array	78.7	Artificial Neural Network (ANN)	HFSS
[17]	Patch antenna	18-24	ANN, Particle Swarm Optimization (PSO)	IE3D
Proposed Design	Rectangular patch antenna	2.45	Linear Regression	HFSS

The high accuracy of ML model predictions suggests that the ML models can effectively capture the complex relationships between design parameters and performance outcomes, enabling designers to optimize antenna characteristics rapidly and with confidence.

5. Conclusion

This paper suggests a successful optimization strategy for the design of rectangular patch antenna structures using linear regression and machine learning. The suggested technique outperforms the prediction of the performance matrix of a patch antenna to speed up the design procedure. The accuracy, consistency, and reliability of the ML models' predictions, as evidenced by the MSE values, further validate their suitability for antenna design optimization. The prediction from the linear regression model is best suited due to its ability to closely replicate the performance metrics (resonant frequency and return loss) compared with HFSS simulation results.

For resonant frequency, the achieved accuracy rates range from 91.94% to 97.18%, with the best model, V3, showing a near-perfect match to the simulated data. In the case of return loss, the accuracy measured from 78.69% to 99.77%, with model V1 being the most precise. This high accuracy indicates that the model can reliably predict the frequency at which the antenna operates most efficiently, which is crucial for ensuring optimal performance in practical applications. Return loss is a measurement of how well the antenna impedance matches the transmission line.

An accurate estimation of this parameter maximizes the effectiveness of the antenna by ensuring that it can transmit signals with the least amount of reflection. The models give engineers a reliable tool to investigate a variety of design configurations without requiring laborious and computationally demanding simulations by reducing the differences between expected and actual values.

Conflicts of Interest

The authors declare no conflict of interest.

References

[1] Yi Qian et al., "The Internet of Things for Smart Cities: Technologies and Applications," *IEEE Network*, vol. 33, no. 2, pp. 4-5, 2019. [CrossRef] [Google Scholar] [Publisher Link]

[2] M. Rezwanul Mahmood et al., "A Comprehensive Review on Artificial Intelligence/Machine Learning Algorithms for Empowering the Future IoT Toward 6G Era," *IEEE Access*, vol. 10, pp. 87535-87562, 2022. [CrossRef] [Google Scholar] [Publisher Link]

[3] Walid Saad, Mehdi Bennis, and Mingzhe Chen, "A Vision Of 6G Wireless Systems: Applications, Trends, Technologies, and Open Research Problems," *IEEE Network*, vol. 34, no. 3, pp. 134-142, 2020. [CrossRef] [Google Scholar] [Publisher Link]

[4] Bo Liu et al., "An Efficient Method for Antenna Design Optimization Based on Evolutionary Computation and Machine Learning Techniques," *IEEE Transactions on Antennas and Propagation*, vol. 62, no. 1, pp. 7-18, 2014. [CrossRef] [Google Scholar] [Publisher Link]

[5] Fahad Shamshad, and Muhammad Amin, "Simulation Comparison between HFSS and CST for Design of Conical Horn Antenna," *Journal of Expert Systems (JES)*, vol. 1, no. 4, pp. 84-90, 2012. [Google Scholar]

[6] Han Zhenhua, and Aidehaijiang Manafu, "Simulation Application of Finite Element Analysis Software HFSS in Antenna Engineering Design Under the Background of Big Data," *2022 International Conference on Inventive Computation Technologies (ICICT)*, Nepal, pp. 710-713, 2022. [CrossRef] [Google Scholar] [Publisher Link]

[7] Md Rayhan Khan et al., "A Generalized Approach to Real-Time Performance Estimation of Antenna Types Using Deep Learning," 2022 *IEEE International Symposium on Antennas and Propagation and USNC-URSI Radio Science Meeting (AP-S/URSI)*, Denver, CO, USA, pp. 497-498, 2022. [CrossRef] [Google Scholar] [Publisher Link]

[8] Naomi Estera Costea, Elisa Valentina Moisi, and Daniela Elena Popescu, "Comparison of Machine Learning Algorithms for Prediction of Diabetes," *2021 16th International Conference on Engineering of Modern Electric Systems (EMES)*, Oradea, Romania, pp. 1-4, 2021. [CrossRef] [Google Scholar] [Publisher Link]

[9] Xiao Hui Chen et al., "A Hybrid Algorithm of Differential Evolution and Machine Learning for Electromagnetic Structure Optimization," *2017 32nd Youth Academic Annual Conference of Chinese Association of Automation (YAC)*, Hefei, China, pp. 755-759, 2017. [CrossRef] [Google Scholar] [Publisher Link]

[10] Daniel R. Prado et al., "Efficient Shaped-Beam Reflectarray Design Using Machine Learning Techniques," *2018 48th European Microwave Conference (EuMC)*, Madrid, Spain, pp. 1545-1548, 2018. [CrossRef] [Google Scholar] [Publisher Link]

[11] Claudio R. M. Silva, and Sinara R. Martins, "An Adaptive Evolutionary Algorithm for UWB Microstrip Antennas Optimization Using a Machine Learning Technique," *Microwave and Optical Technology Letters*, vol. 55, no. 8, pp. 1864-1868, 2013. [CrossRef] [Google Scholar] [Publisher Link]

[12] Carmine Gianfagna et al., "Enabling Antenna Design with Nano-Magnetic Materials Using Machine Learning," *2015 IEEE Nanotechnology Materials and Devices Conference (NMDC)*, Anchorage, AK, USA, pp. 1-5, 2015. [CrossRef] [Google Scholar] [Publisher Link]

[13] Lorenza Tenuti et al., "Advanced Learning-Based Approaches for Reflectarrays Design," *2017 11th European Conference on Antennas and Propagation (EUCAP)*, Paris, France, pp. 84-87, 2017. [CrossRef] [Google Scholar] [Publisher Link]

[14] Carmine Gianfanga et al., "Machine-Learning Approach for Design of Nanomagnetic-Based Antennas," *Journal of Electronic Materials*, vol. 46, no. 8, pp. 4963-4975, 2017. [CrossRef] [Google Scholar] [Publisher Link]

[15] Nurhan Türker Tokan, and Filiz Gunes, "Support Vector Characterization of the Microstrip Antennas Based on Measurements," *Progress in Electromagnetics Research B*, vol. 5, pp. 49-61, 2008. [CrossRef] [Google Scholar] [Publisher Link]

[16] Jinpil Tak et al., "A 3-D-Printed W-Band Slotted Waveguide Array Antenna Optimized Using Machine Learning," *IEEE Antennas and Wireless Propagation Letters*, vol. 17, no. 11, pp. 2008-2012, 2018. [CrossRef] [Google Scholar] [Publisher Link]

[17] Satish K. Jain, "Bandwidth Enhancement of Patch Antennas Using Neural Network Dependent Modified Optimizer," *International Journal of Microwave and Wireless Technologies*, vol. 8, no. 7, pp. 1111-1119, 2016. [CrossRef] [Google Scholar] [Publisher Link]

[18] Anshuman Garg, and Anjana Goen, "Substrate Height and Dielectric Constant Dependent Performance of Rectangular Micro Strip Patch Antenna," *International Journal of Electrical & Electronics Research (IJEER)*, vol. 2, no. 3, pp. 36-39, 2014. [CrossRef] [Google Scholar] [Publisher Link]

[19] Ja-Hao Chen, and Chen-Yang Cheng, "Multiple Performance Optimization for Microstrip Patch Antenna Improvement," *Sensors*, vol. 23, no. 9, pp. 1-10, 2023. [CrossRef] [Google Scholar] [Publisher Link]

[20] Nayan Sarker et al., "Applications of Machine Learning and Deep Learning in Antenna Design, Optimization, and Selection: A Review," *IEEE Access*, vol. 11, pp. 103890-103915, 2023. [CrossRef] [Google Scholar] [Publisher Link]

[21] Yang Zhong et al., "A Machine Learning Generative Method for Automating Antenna Design and Optimization," *IEEE Journal on Multiscale and Multiphysics Computational Techniques*, vol. 7, pp. 285-295, 2022. [CrossRef] [Google Scholar] [Publisher Link]

[22] Yitong Liu et al., "Real-Time 3-D MIMO Antenna Tuning with Deep Reinforcement Learning," *IEEE Transactions on Cognitive Communications and Networking*, vol. 8, no. 2, pp. 1202-1215, 2022. [CrossRef] [Google Scholar] [Publisher Link]

[23] Yiming Chen, Atef Z. Elsherbeni, and Veysel Demir, "Machine Learning for Microstrip Patch Antenna Design: Observations and Recommendations," *2022 United States National Committee of URSI National Radio Science Meeting (USNC-URSI NRSM)*, Boulder, CO, USA, pp. 256-257, 2022. [CrossRef] [Google Scholar] [Publisher Link]

[24] Mina Malekzadeh, "Performance Prediction and Enhancement of 5G Networks based on Linear Regression Machine Learning," *EURASIP Journal on Wireless Communications and Networking*, vol. 2023, no. 1, pp. 1-34, 2023. [CrossRef] [Google Scholar] [Publisher Link]